

Application of Principles for Fracture-Safe Design for Aluminum and Titanium Alloys

An interpretation of the principles and procedures that have been evolved for predicting flaw size/stress level conditions for fracture

BY R. J. GOODE AND R. W. JUDY, JR.

ABSTRACT. This report summarizes fracture resistance characterization information for high and ultrahigh strength aluminum alloys and titanium alloys and presents the procedures that have been evolved for translating this information into structural mechanics predictions for fracture.

Dynamic Tear (DT) and K_{Ic} test methods have been used to establish the fracture resistance characterizations for material covering a wide range of yield strength and metallurgical conditions. Ratio Analysis Diagram (RAD) procedures provide the structural performance predictions.

Introduction

The interest in use of high strength aluminum and titanium alloys for structural applications is due primarily to their high strength-to-density ratio. Other factors relate to good oxidation and corrosion characteristics for specific alloys as well as non-magnetic properties. However, an important factor in reliable fracture-safe utilization of these materials is knowledge of their fracture resistance characteristics. Meaningful fracture resistance information for the full strength spectrum of titanium and

aluminum alloys has only been developed in the last few years. This report summarizes the fracture resistance characterization information for these materials commercially produced as large plates and presents the procedures that have been evolved for translating this information into meaningful predictions of flaw size-stress level conditions for fracture. These procedures are similar to those evolved for control of fracture in structures of high and ultrahigh strength steels (Ref. 1).

Appendix Tables A1 and A2 list the various alloys and range of properties studied.

Fracture Mode Characteristics

The final event of structural failure is rapid separation-fracture. Various laboratory tests have been evolved to study fracture. Each of these has a specific application, which is determined by the fracture state. The full range of fracture states extends from glass-like brittleness to high ductility; the important engineering reference points are the dividing lines or limits separating the three fracture states (Fig. 1):

● Brittle behavior (plane strain) as illustrated at the bottom of the figure can be viewed as the unstable

LIST OF SYMBOLS

DT	= Dynamic Tear (test)
K	= Stress intensity factor
K_{Ic}	= Critical value of K for plane strain crack extension at slow loading rates
RAD	= Ratio Analysis Diagram
Ratio	= Refers to lines of constant K_{Ic} / σ_{ys} on the RAD
σ_{ys}	= Yield strength of material
R	= Resistance to fracture extension
C_v	= Standard Charpy-V notch test
B	= Thickness dimension of specimen or plate
EB	= Electron beam
ETT	= Explosion Tear Test
TL	= Technological Limit
GFM	= Graphical Fracture Mechanics
α	= Alpha, low temperature close-packed hexagonal phase of titanium
β	= Beta, high temperature body-centered cubic phase of titanium

R. J. GOODE and R. W. JUDY, JR. are associated with the Strength of Metals Branch, Metallurgy Division, Naval Research Laboratory, Washington, D.C.

propagation by elastic stress fields with minimal attendant deformation or plasticity at the crack tip. States 1 and 2 refer to high and low levels of resistance to the initiation of unstable fractures.

- Crack extension under elastic-plastic conditions (middle figure) connotes crack propagation processes at high elastic stress levels with appreciable crack tip plasticity. Fracture states 3 and 4 refer respectively to low and high elastic stress requirements for propagation of through-thickness cracks.

- Ductile (plastic) crack extension processes (top) involve stresses over yield, high crack tip ductility and consequent high energy expenditure to "drive" the crack. Furthermore, in the first stages of crack extension, energy requirements to support crack growth increase rapidly so that a natural crack arresting condition is present for elastic stress fields. Fracture states 5 and 6 refer respectively to low and high energy requirements to sustain stable crack extension at over-yield stress levels.

Titanium and aluminum alloys are considered "strength transition" materials. Only a gradual rise in fracture resistance with increasing temperature is featured for high strength titanium alloys; for high strength aluminum alloys there is essentially no effect of increasing temperature on fracture resistance. This behavior is contrasted to the abrupt increase in fracture resistance for the low and intermediate strength, temperature transition steels, Fig. 2. The macrofracturing process for all conditions of fast fracture in titanium and aluminum alloys is one of microvoid coalescence of the metal where brittle, intermetallic or precipitate particles fracture in advance of a moving crack forming microcracks in the material. The microcracks enlarge creating voids (dimples) of a size proportional to the matrix ductility (fracture toughness) of the material. This fracture mode is illustrated in Fig. 3.

The increase in dimple size with increasing fracture toughness, relates to increased resistance of the metal to extension of a crack. The fracture extension resistance process can be visualized in terms of a resistance (R) curve, which corresponds to the increase in plastic work absorbed per unit increment of initial fracture extension. No increase in plastic work energy absorption is required for fracture extension in the brittle (very small dimple) case. Initial instability of the crack results in fracture propagation through the total section of material without any requirement for further increase in nominal elastic stress level. Thus, the R curve is flat for brittle titanium and aluminum alloys.

For the ductile fracture case, an increase in plastic work energy is required with initial crack extension. The amount of increase, R-curve slope, is proportional to the intrinsic ductility of the metal.

At this point the reader is referred to Refs. 2 and 3 for detailed discussions of the relationships of R-curve slope to fracture state, crack tip plastic zone size, crack-tip-plasticity conditions, metal ductility range, and section size effects involved in characterization of fracture resistance. Propelling force aspects that relate to structural considerations are also covered in the above references.

The R-curve slope characteristics for plane strain and high plastic fracture resistance of aluminum and titanium alloys are shown in Figs. 4 and 5, respectively. These curves were developed by modeling the fracture-extension process using DT test specimens of different crack lengths. The two test series for each material feature the same characteristics that have been shown for steels (Ref. 2). A flat R curve is characteristic for brittle alloys and a steeply rising R curve characterizes the highly ductile alloys. Intermediate and low R-curve slopes are obtained for materials of intermediate and low fracture extension resistance.

Fracture Resistance Tests for Aluminum and Titanium

The principal laboratory tests that have been used to measure the fracture resistance characteristics of aluminum and titanium alloys include the DT, K_{Ic} , C_v (titanium), and notched tensile ratio (aluminum) methods. However, work at NRL dur-

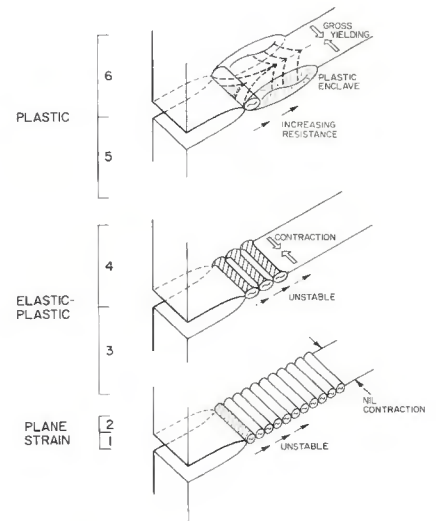


Fig. 1 — Illustration of the three fracture states for high strength metals

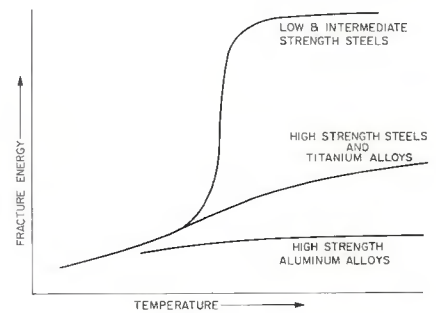


Fig. 2 — Schematic illustration of the general effect of temperature on resistance characteristics of structural metals

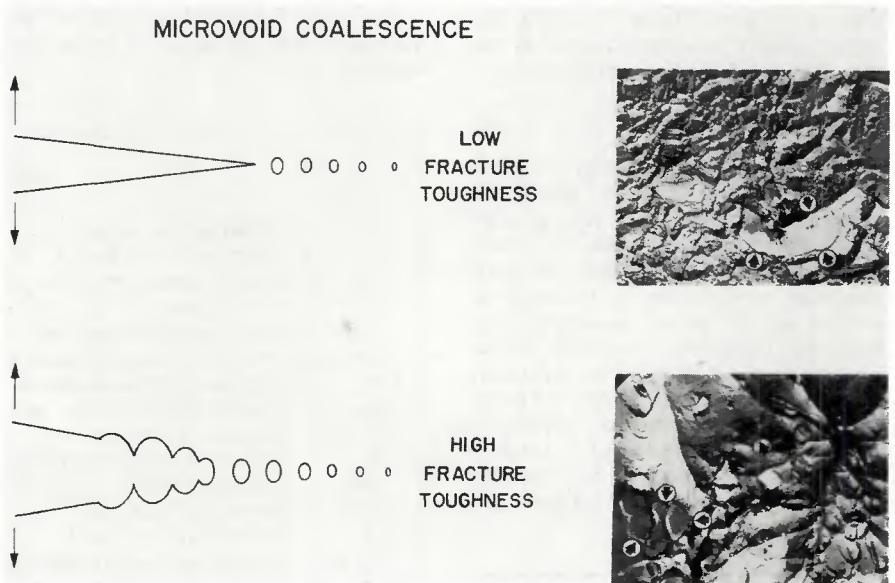


Fig. 3 — Illustration of the effect of increasing fracture resistance on microvoid coalescence processes. The arrows in the microfractographs indicate "brittle" particles which fracture ahead of the advancing crack front causing unit action of the void formation process. The size of the voids (dimples) is an index of the microfracture ductility of the matrix material

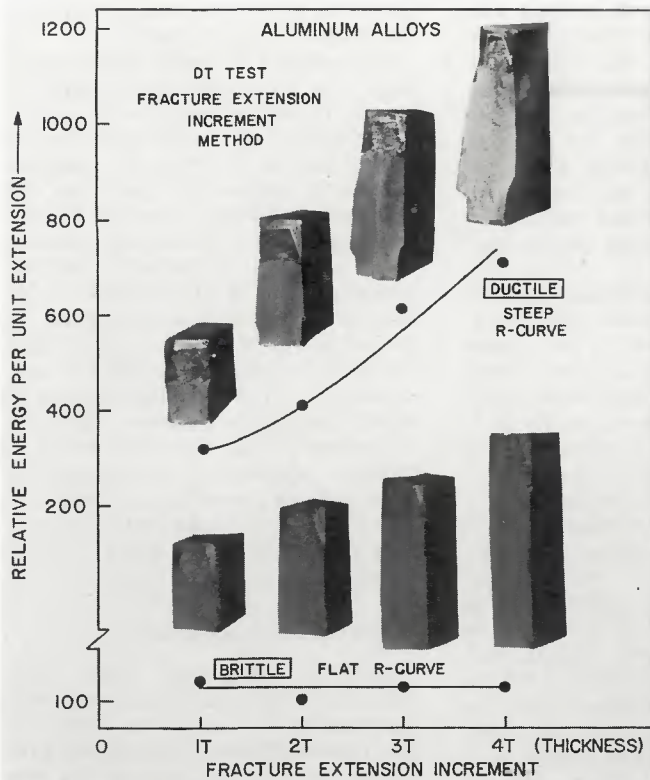


Fig. 4 — Representative R curve slopes for brittle and ductile aluminum alloys in 1 in. thickness. The relative increase in plastic work energy for fracture extension is modeled by Dynamic Tear (DT) test specimens of increasing fracture path lengths. The increased lengths provide for measurement of the effects of decreased triaxial constraint in the process of fracture extension

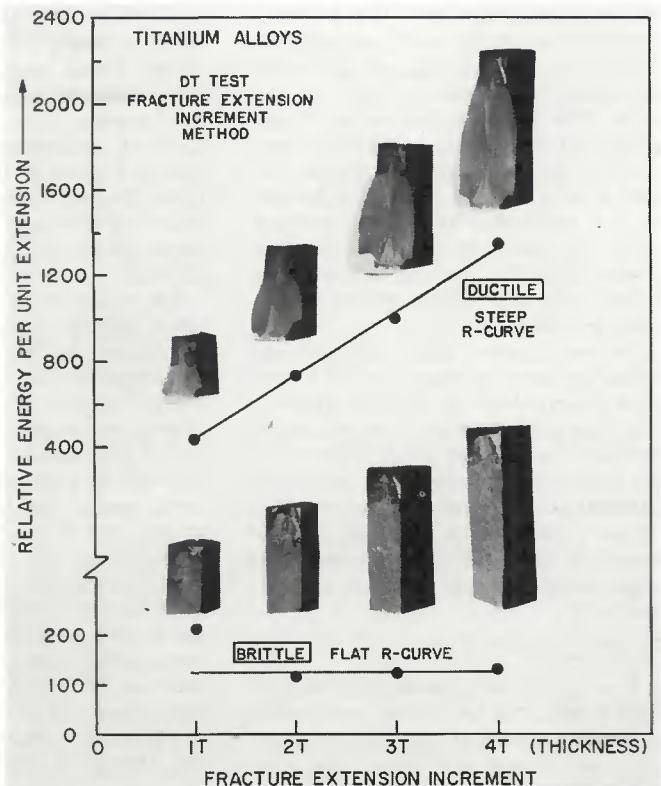


Fig. 5 — Representative R curve slopes for brittle and ductile titanium alloys of 1 in. thickness

ing the last five years established the fact that only results of DT and K_{Ic} tests provide reliable definition of levels of fracture toughness in these materials.

Fracture Mechanics Tests

Fracture mechanics tests characterize fracture resistance in terms of the value of the elastic stress field intensity K in the region ahead of the crack tip plastic zone. The critical stress-intensity level for crack extension (instability) is designated by the parameter K_{Ic} . The subscript I defines the condition of the opening mode for which the applied stress is normal to the plane of the crack.

The K_{Ic} value must be determined under the condition of plane strain (maximum possible mechanical constraint that can be applied to the metal at the crack tip). The K_{Ic} value represents the lowest value of fracture resistance and is considered to be geometry independent. Plane strain is attained in K_{Ic} testing by imposing predetermined requirements on the width, length, thickness, and crack depth of the fracture mechanics specimens to ensure that minimum i.e., valid K_{Ic} values are obtained. Of these dimensions, thickness is most significant to valid K_{Ic} determina-

tions, because it is the basic dimension from which the other dimensions required for maximum mechanical constraint are determined. For example, an increase in thickness is required with an increase in fracture resistance to simultaneously maintain flaw width and depth dimensions sufficient to maximize constraint conditions at the crack tip.

Once a valid plane strain K_{Ic} value has been established, it is then possible to calculate critical flaw size-stress level relationships for various kinds of flaws in the material, based on equations derived by linear-elastic fracture mechanics. The calculations, therefore, presuppose that equivalent conditions of maximum constraint are involved. To ensure that the requirements for plane strain (Ref. 4) can be met, the thickness of the K_{Ic} specimen must satisfy the conditions

$$B \geq 2.5 (K_{Ic} / \sigma_{ys})^2,$$

where

B = thickness (in.)

K_{Ic} = critical plane strain stress-intensity factor (ksi $\sqrt{\text{in.}}$),

and

σ_{ys} = yield stress (ksi).

It is important to note that the ratio

of $(K_{Ic} / \sigma_{ys})^2$ is proportional to the crack-tip plastic zone size. According to this ratio, a specific K_{Ic} value related to metal of increased yield strength results in a decrease in the plastic zone size, i.e., a decrease in fracture resistance. An increase in the K_{Ic} value for a given level of yield strength corresponds to a rapid increase in the plastic zone size and the $(K_{Ic} / \sigma_{ys})^2$ ratio and, therefore, the B requirement for retention of the plane strain condition. Consequently, for materials of high fracture resistance the required specimen size becomes very large. For example, a material with a ratio of 2.0 requires a B (test thickness) value of at least 10 in.

If the thickness is less than the minimum B requirement, the mechanical constraint is then less than adequate for plane strain, even for a very deep crack; thus, the measurement of fracture resistance must involve procedures that relate to defining fracture extension resistance characteristics.

Values of K are calculated from experimental determination of crack tip opening displacements obtained by means of a clip gage spanning the crack opening. Load-clip gage displacement plots provide the indication of a crack-tip opening instability by a drop in the load with increasing

clip gage displacement. The nominal stress is calculated using appropriate equations. The critical stress-intensity factor for instability, K_{Ic} , is derived from fracture mechanics equations that relate K to crack depth and nominal stress. Crack instability occurs at a value of K_{Ic} which is unique to the material. Different combinations of crack depth and nominal stress can be used to obtain this value, provided plane strain conditions are satisfied.

At the present stage of development, fracture mechanics tests do not lend themselves to routine testing. The cost of K_{Ic} testing is high, due to the requirement of close tolerances on specimen dimensions, stringent conditions for producing acceptable fatigue cracks, and other aspects of research laboratory equipment and procedures required in the conduct of the tests.

Dynamic Tear (DT) Test

The DT test was developed to provide a practical laboratory procedure for measurement of the fracture resistance associated with the characteristic fracture propagation mode of the metal. A principal requirement for this purpose, which is a feature of the DT test, is the simulation of a deep, sharp crack for the initiation of the fracture. This feature is obtained for the DT test by introducing an electron beam (EB) weld embrittled with iron (for titanium specimens) or phosphor bronze (for aluminum), thereby eliminating the complications of fatigue precracking.

Recently, it was established that equivalent results could be obtained by use of a deep, sharp crack produced by use of a machined or slot notch sharpened at the tip by a pressed knife edge (Ref. 5). The energy required to fracture the specimen serves as an index of the size of the crack-tip plastic zone associated with the natural process of fracture propagation. The width-to-thickness geometry of the DT test is sufficient to establish conditions for the development of the natural fracture mode related to intrinsic fracture resistance and thickness aspects.

For relatively brittle materials, which fracture in the plane strain mode (flat fracture) with small plastic zones, low energy absorption is measured. With increasing resistance to fracture the plastic zone size increases, culminating in the development of a large plastic enclave preceding the fracture process. At high fracture energies, slant fracture (shear) is generally obtained. Mechanical constraint effects due to thickness, which influence the plastic zone size, may be evaluated directly by scaling the size of the DT specimen.

In effect, the DT test defines the fracture mode (plane strain, mixed-mode plane stress, or full plane stress) when conducted for the specific section size of interest. The effects of deviations from the specific size (DT tests of thickness less than plate thickness) may be interpreted from the intrinsic fracture resistance value and fracture mode that is observed.

For example, a flat-break fracture which implies plane strain conditions would not be changed by increased thickness. Similarly, a full-slant plane stress fracture, associated with high energy absorption measured for a 1 in. DT test specimen, implies that an increase to sections of 2 to 3 in. thickness would not be expected to decrease the fracture resistance level significantly for the same metallurgical condition. Thus, the characterization of the thick-section fracture resistance as related to gross strain mechanical conditions would not change. For intermediate fracture resistance levels represented by mixed-mode plane stress fractures, the effects of changes in section size require more detailed assessment for

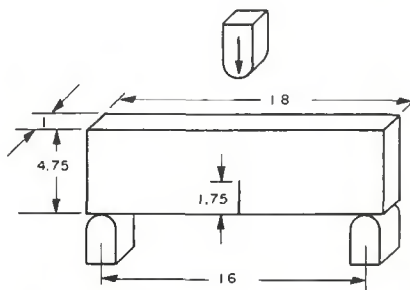


Fig. 6 — Standard 1 in. DT specimen featuring a 1.75 in. deep electron beam brittle weld crack starter

purposes of engineering interpretation to specific applications.

A schematic drawing of the standard 1 in. DT specimen is shown in Fig. 6. Impact loading with a calibrated falling or swinging pendulum weight (similar to a large C_v machine) is used to fracture the specimen and measure the energy required to fracture a specified area of plate material.

An example of fracture surface characteristics of DT specimens for extremes in fracture toughness is shown in Fig. 7 for aluminum alloys and titanium alloys. The flat fracture, indicated on the left, corresponds to brittle (plane strain) behavior and low DT energy values. Very high levels of fracture resistance correspond to conditions of plane stress for which high DT energy values and slant fracture, indicated on the right, are obtained.

C_v and Notched Tensile Tests

The C_v test has been used extensively by industry and research laboratories for measuring the fracture energy of titanium alloys. As a result of work at NRL during the late 1960's, the C_v test has been demonstrated to lack adequate discrimination capabilities between different levels of fracture resistance. This inadequacy is due to the blunt notch and lack of specimen depth adequate to establish the characteristic fracture mode. These deficiencies are manifested in C_v data that did not reliably indicate the true level of fracture resistance of the material tested. Further, the C_v test often erroneously indicates increasing fracture resistance (as a result of heat treatment, different processing, etc.) compared to the DT, K_{Ic} and structural prototype tests. The DT test and K_{Ic} test (where

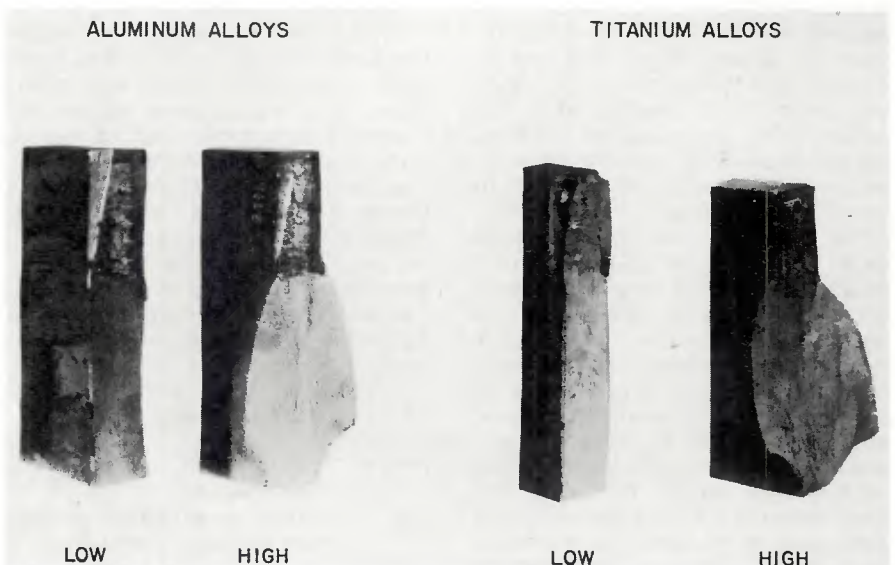


Fig. 7 — Features of Dynamic Tear (DT) test fracture surface for aluminum and titanium alloys of low and high fracture toughness

appropriate) are now being used to provide the major guidance for such studies.

The aluminum industry has long recognized the inadequate discrimination capability of the C_v test for aluminum alloys. In general the C_v test is relatively insensitive to changes in fracture resistance, and

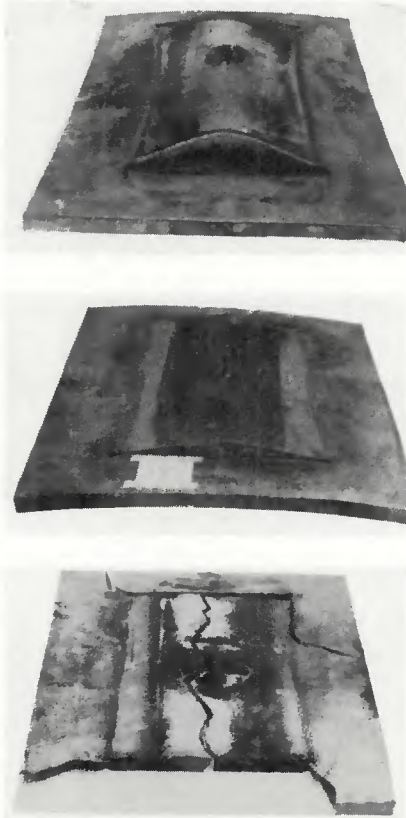


Fig. 8 — Series of Explosion Tear Test (ETT) plates illustrating the structural prototype performance of high, intermediate, and low fracture resistance (top to bottom) as measured by DT tests

the total range of fracture energy for the spectrum of aluminum alloys corresponds to low values.

Thus, for many years the principal method for fracture resistance evaluation of aluminum alloys has been based on tests of notched round tensile bars. The parameter of fracture resistance comparison is the ratio of the breaking strength of the notched bar to the tensile yield strength of the material, for a specific notch acuity. Increasing values of the ratios above 1.0 were considered to indicate increasing ability for the material to plastically deform at the notch tip. Although, compared to the C_v test, this test was felt to provide better discrimination capability for changes in fracture resistance, the improvement was not great.

Other difficulties, which were also a result of the wide variety of notched tensile specimen geometrics and notch acuities used, related to translation of the variety of ratio values obtained for a material to a specific level of fracture resistance and to structural performance. At the present time, different configurations of the notched tensile test specimen are being studied by a Subcommittee of ASTM Committee E-24 on Fracture for possible standardization.

Correlations of DT and K_{Ic} Fracture Resistance Tests

Early interpretations of DT and K_{Ic} data depended on extensive indexing of the results of the Explosion Tear Test (ETT). The ETT is a prototype structural element test designed to simulate elastic and/or plastic loading of a flawed panel of prime plate material. Explosive loading methods are employed to deform the 22 × 25 × 1 in. thick test panel into

a cylindrical form with the primary stress being normal to a centrally located flaw. A 2 in. long, through-thickness, embrittled EB weld, similar to the DT crack-starter weld, initiates a propagating crack into elastically or plastically loaded material, depending on fracture resistance. The indexing parameter of the ETT is the amount of surface plastic strain required to cause extensive fracture of the test piece.

Thus, the ETT yields an indication of the material's tolerance for large flaws. The typical performance of high, intermediate, and low fracture resistance material is shown in Fig. 8 for titanium alloys. The fracture modes (top to bottom) correspond, respectively, to plane stress mixed-mode plane stress, and full plane strain. Similar performance is displayed by aluminum alloys for the same fracture modes.

DT- K_{Ic} Correlations

The recently developed DT- K_{Ic} correlations for aluminum and titanium alloys provided for a major advancement in the interpretation of fracture resistance data for fracture-safe design with these materials. Translation of the DT energy data into flaw size-stress level conditions for fracture for the plane strain case could be made from the correlations. The DT- K_{Ic} correlations shown in Figs. 9 and 10 for aluminum and titanium alloys, respectively, illustrate that for increasing K_{Ic} values there is a corresponding increase in DT energy values. However, for the 1 in. thick (full plate thickness) specimen tested, valid K_{Ic} values obtained were limited to about 30 $\text{ksi}\sqrt{\text{in.}}$ and 85 $\text{ksi}\sqrt{\text{in.}}$ for aluminum and titanium alloys of about 50 $\text{ksi } \sigma_{ys}$ and 130 ksi

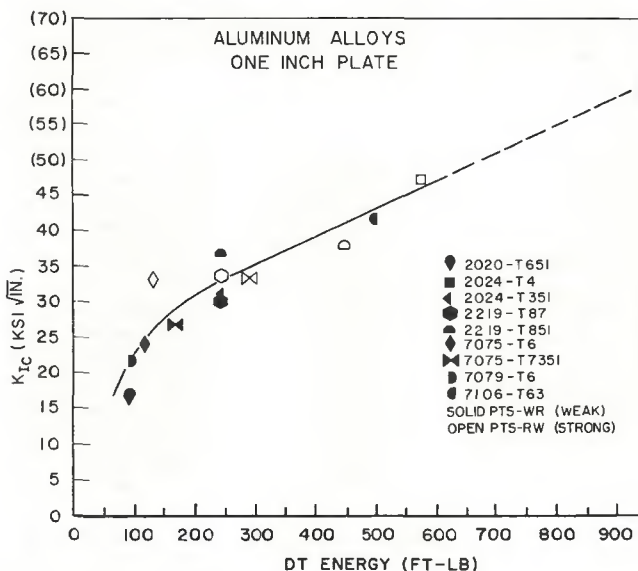


Fig. 9 — Relationship of K_{Ic} to DT energy for aluminum alloys

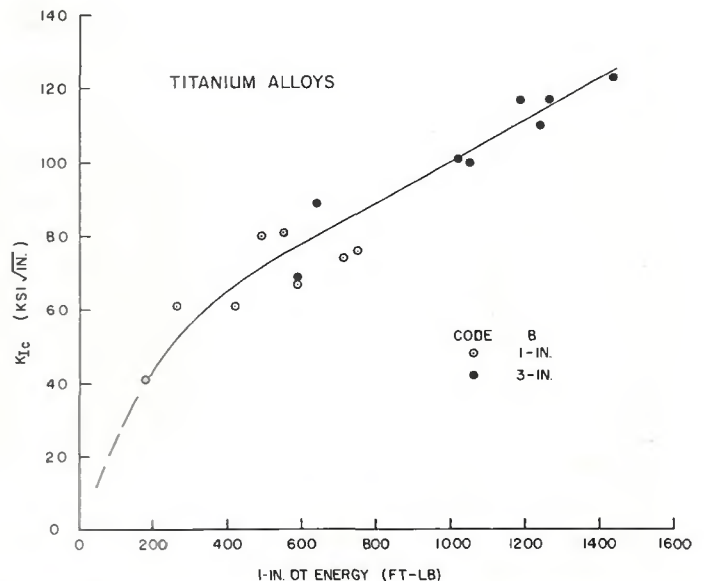


Fig. 10 — Relationship of K_{Ic} to DT energy for titanium alloys

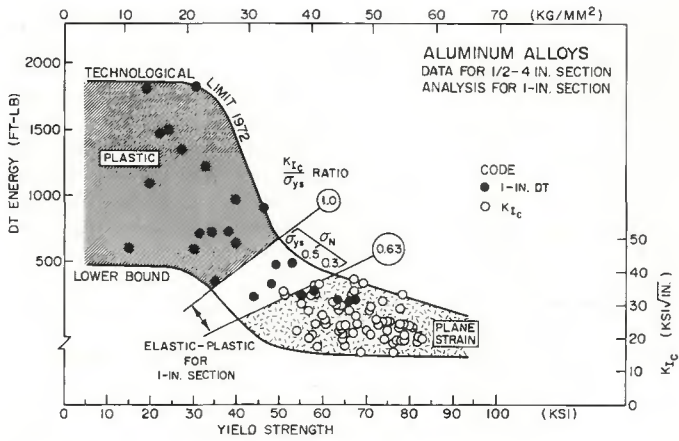


Fig. 11 — Summary of K_{Ic} and Dynamic Tear (DT) test data for a variety of aluminum alloys

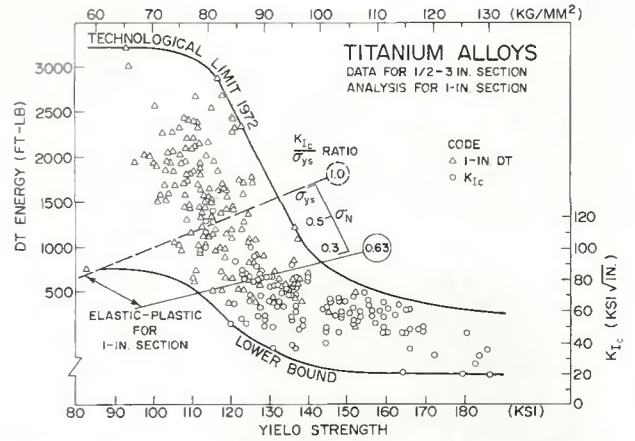


Fig. 12 — Summary of K_{Ic} and Dynamic Tear (DT) test data for titanium alloys produced as plates of 1 to 3 in. thickness. The alloys feature variations in chemistry, processing and heat treatment

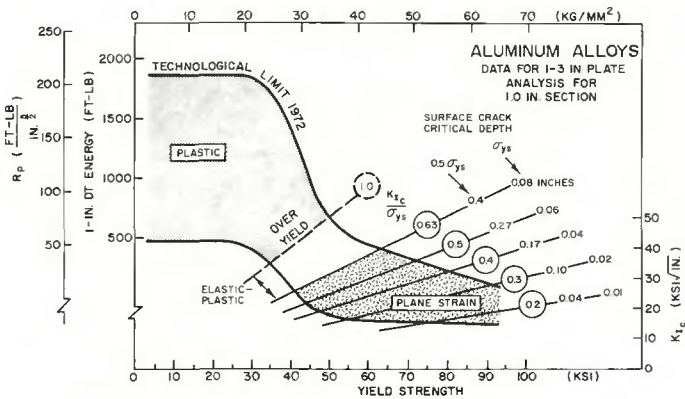


Fig. 13 — Ratio Analysis Diagram (RAD) for aluminum alloys produced in 1 to 3 in. plate thickness. The RAD combines the metal data bank summarization (TL and lower bound lines) with a structural mechanics interpretative system defining critical fracture conditions based on K_{Ic} / σ_{ys} ratio lines

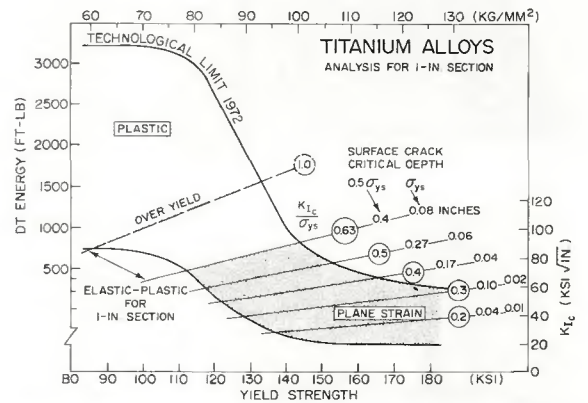


Fig. 14 — RAD for high strength titanium alloys produced in 1 to 3 in. plate thickness

σ_{ys} respectively, according to current ASTM E399-72 criteria (Ref. 4).

Ratio Analysis

The basic data which led to development of RAD diagrams for 1 in. thick plate material are shown in Fig. 11 for aluminum alloys and Fig. 12 for titanium alloys. The upper limit of highest metallurgical quality material as defined by fracture resistance properties is represented by the TL (Technological Limit) curve. A similarly defined curve relating to the lowest metallurgical material is represented by the lower bound curve. The limit curves are indexed by DT energy values for the ductile materials, and by K_{Ic} data for the plane strain materials. The data points represent the latest (1972) DT and K_{Ic} information evolved from metallurgical research studies at NRL and at other research laboratories (K_{Ic} data only).

Note that for each alloy system there is a relatively narrow yield strength range over which the TL trend line drops sharply from a high level of obtainable fracture resistance

to a low level of resistance. This sharp drop, which occurs at 30-50 ksi yield strength for aluminum alloys and 120-140 ksi yield strength for titanium alloys, defines the strength transition range for the best quality material. A series of similar curves could be drawn for intermediate levels of metallurgical quality, which would fall between the TL and lower bound lines. Decreasing metallurgical quality causes a downward shift of the strength transition to a lower range of yield strength.

The relative position of the DT and K_{Ic} scales on these plots is provided by the DT- K_{Ic} correlation plots described earlier. The relationship of K_{Ic} to yield strength locates the K_{Ic} / σ_{ys} ratio lines on the plot for translation of DT and K_{Ic} data to critical flaw size-stress level predictions, as described below. The 0.63 ratio line, noted in Figs. 11-12, relates to the upper limit of plane strain for a 1 in. section thickness.

Ratio Analysis Diagrams for Aluminum and Titanium Alloys

The K_{Ic} / σ_{ys} Ratio Analysis Di-

agrams (RAD's) for high-strength aluminum and titanium alloys are shown in Figs. 13 and 14, respectively. These diagrams combine the metallurgical information (TL and lower bound lines) with a structural mechanics interpretative system of critical flaw size-stress level for fracture based on a system of K_{Ic} / σ_{ys} ratio lines. The critical flaw size noted for yield and 0.5 yield strength at each ratio level was obtained using the Graphic Fracture Mechanics (GFM) plot, Fig. 15, for a long, thin surface flaw in a tensile stress field. The GFM procedures are discussed in detail in Ref. 2.

The ratio lines also divide the diagram into regions of expected plastic, brittle, and elastic-plastic behavior for given material thicknesses. The separations are determined according to thickness as shown for 1 in. section size in Figs. 12-14. The critical edge between brittle behavior and elastic-plastic behavior is the plane strain limit. The boundary between the elastic-plastic and ductile regimes is the general yield limit. The division of the RAD into three regions

provides an engineering index of the fracture state and thereby serves to indicate the type of more detailed design approach required for each case.

The RAD is a "plotting board" for analysis of combined strength and fracture resistance properties of materials in relation to specific structural mechanics problems. Effects of variability of materials properties and minimum strength specifications for particular structures are readily analyzable. Additionally, effects of crack growth by fatigue and SCC processes are made readily apparent by RAD procedures. A more detailed explanation of the RAD can be found in Ref. 3.

Compendium RAD's, which summarize all the fracture resistance data for the generic families of aluminum and titanium, are presented in Figs. 16 and 17 respectively. The zonal locations for each family are based on all available DT and K_{Ic} data and cover the yield strength and fracture resistance range generally encountered with current alloys and processing techniques.

Aluminum Alloys

The general fracture toughness characteristics of each aluminum alloy family is indexed on the RAD in Fig. 16. For example, the DT zonal location of the 5000 series alloys in the plastic region indicates very high fracture resistance capabilities (high R curve slope) for these alloys below 40 ksi yield strength. Thus, large to huge size flaws and general plastic yielding are required for fracture. The 5000 series alloys define the TL line up to about 35 ksi yield strength. Due to the metallurgical nature of these alloys, yield strengths much above 45 ksi would be difficult to obtain in thick sections.

Alloys in the 6000 series can be expected to span the yield strength range of about 20 to 65 ksi depending on the chemistry and tempering treatment. The 6061 alloy in the T651 temper is the only one of this family for which DT data are available. The alloy has a yield strength around 40 ksi for this temper condition and a level of fracture resistance below that

of the TL line but still in the plastic region where intermediate R curve slope would be expected.

The 2000 series alloys are designed for the general yield strength ranges of 40 to 65 ksi and from RAD definitions would be expected to be plane strain at the higher end of this range. Low R curve slope characteristics would be expected for 2000 series alloys at the low end of the strength range for 1 in. thick sections.

In general, only alloys in the 7000 series are used above 65 ksi yield strength. These alloys are the high strength aircraft alloys, such as 7075, and are relatively brittle even for thicknesses significantly less than 1 in. The special-purpose 7000 series alloys designed for use at lower strength levels define the lower strength portion of the DT zonal region. In the region of rapid TL line transition, intermediate levels of fracture resistance for these special purpose alloys may be possible provided close control of chemistry and processing practice is exercised.

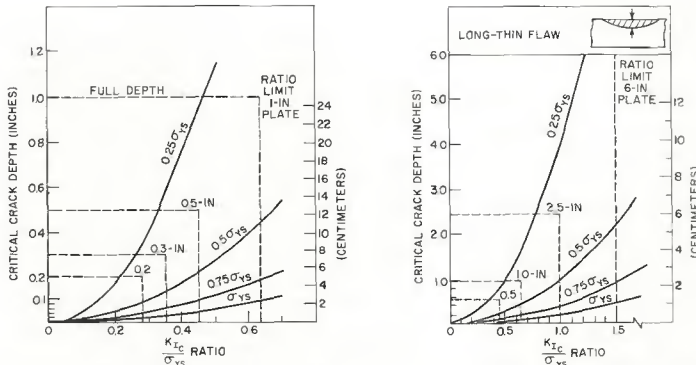


Fig. 15 — Graphical Fracture Mechanics (GFM) plot of critical crack depth versus K_{Ic} / σ_{ys} as a function of nominal tensile stress relative to yield strength, for the case of long-thin surface flaw geometry. The vertical dashed lines indicate the upper ratio limit for plane strain for the specified section thickness

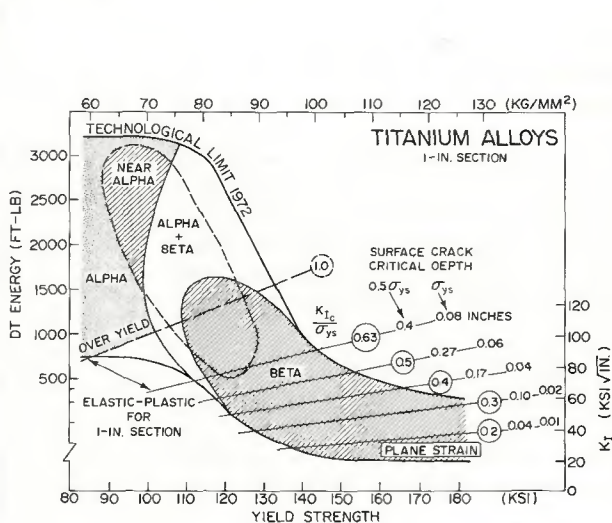


Fig. 17 — RAD for generic families of structural titanium alloys

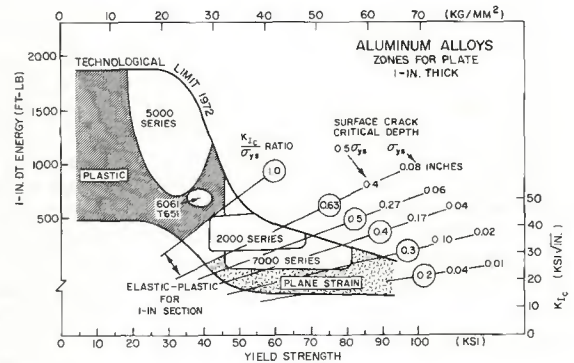


Fig. 16 — RAD for generic families of structural aluminum alloys

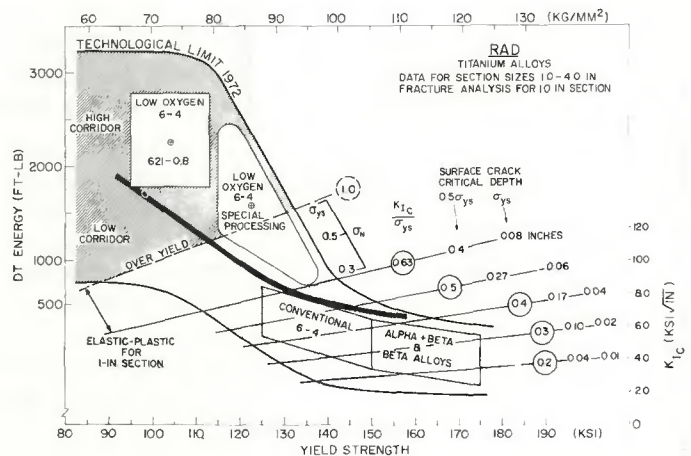


Fig. 18 — RAD for titanium alloys illustrating the strong effect of interstitial oxygen content on both strength and fracture resistance. The dark band separates standard commercial products from plate materials produced with oxygen content of 0.08% or less

Titanium Alloys

The compendium RAD for titanium, Fig. 17, summarizes all fracture resistance information for the generic families of titanium alloys.

Technological Limit line quality material is obtained with α and near- α alloys up to about 100 ksi yield strength. Above 100 ksi yield strength, the fracture resistance of both types of α alloys begins to fall rapidly away from the TL line and optimum properties are no longer obtainable. This rapid drop in fracture resistance for these alloys is illustrated by the upper zone region dropping from the TL line at about 100 ksi yield strength to below the 1.0 ratio line at about 130 ksi yield strength.

Alloys of the $\alpha + \beta$ type define the TL line from 110- to about 190 ksi yield strength.

The β alloys are also expected to follow the TL line in the ultrahigh yield strength range. Limited data for several β alloys indicate that in the lower yield strength range of 110 to 130 ksi, the level of fracture resistance will be below that of the best $\alpha + \beta$ alloys but that K_{Ic} / σ_{ys} ratios of above 1.0 should be obtainable.

Many titanium alloys are capable of a wide range of yield strength and fracture resistance (plastic to plane strain) properties as a result of heat-treating, processing, and chemistry factor variations. Figure 18 presents available yield strength and DT fracture resistance information for several near- α and $\alpha + \beta$ alloys representing commercial practice for 1 in. thick plate. For each alloy shown, a wide variety of metallurgical factor variations have been studied to establish the zonal regions defining the yield strength and fracture resistance limits. Details concerning the specific

processing, heat treatment and chemistry variations studied for each alloy and resultant data obtained are beyond the scope of this report.

Summary

Fracture mechanics analytical procedures provide for characterizing the fracture toughness of high strength titanium and aluminum alloys in terms of critical flaw size-stress level for fracture. However, quantitative characterizations are restricted to relatively brittle alloys at the present state of development of fracture mechanics. These restrictions derive from the transition from plane strain to plane stress as fracture resistance is increased with retention of section size. For both aluminum and titanium alloys, the DT test provides for full spectrum definition of fracture resistance.

Interpretive procedures are evolved from the correlation of K_{Ic} with the DT test for 1 in. and 3 in. thick plates. In the region of low fracture resistance corresponding to a condition of high mechanical constraint (plane strain), the correlations are reasonably accurate.

Fracture resistance data which summarize all information available for 1 in. thick plate in terms of DT energy and K_{Ic} values were presented. The DT energy is indexed to K_{Ic} according to the correlation plot. A TL curve indicating the highest level of fracture resistance attained for any level of yield strength is defined by the DT and K_{Ic} data. Similarly, a lower bound curve defines the lowest level of fracture resistance observed for commercial material. A dramatic drop of the TL line from high to low

fracture resistance in a relatively narrow range of yield strength characterizes the strength transition behavior of these materials.

The K_{Ic} scale on the diagram provides for translation of the DT and K_{Ic} data to flaw size-stress definitions for fracture initiation. This is expressed in terms of K_{Ic} / σ_{ys} ratio lines, which relate to flaw size calculations for the case of plane strain fracture. For the elastic-plastic and plastic regions of the RAD, DT energy corresponds to increasing fracture extension resistance as defined by R curve slope. Critical flaw size determinations cannot be made for this region since fracture mechanics K_{Ic} procedures do not apply. However, increasing R curve slope signifies rapidly increasing resistance to ductile fracture for large flaws.

The spectrum of commercial aluminum and titanium alloys covers a wide range of fracture resistance. Compendium RAD diagrams are presented to summarize the current strength and fracture resistance limitations for generic families of aluminum and titanium.

References

1. Pellini, W. S., "Evolution of Engineering Principles for Fracture-Safe Design of Steel Structures," NRL Report 6957, September 23, 1969.
2. Pellini, W. S., "Integration of Analytical Procedures for Fracture-Safe Design of Metal Structures," NFL Report 7251, March 26, 1971.
3. Pellini, W. S., "Criteria for Fracture Control," NRL Report 7406, May 11, 1972.
4. "Standard Method of Test for Plane-Strain Fracture Toughness of Metallic Materials," ASTM Designation E399-72, Part 31, ASTM Standards, pp. 955-963.
5. Lange, E. A., Puzak, P. P. and Cooley, L. A., "Standard Method for the 5/8 Inch Dynamic Tear Test," NRL Report 7159, August 27, 1970.

SOLDERING MANUAL

*A 170-page hard cover book
that will tell you how, when
and what to solder*

The SOLDERING MANUAL consists of 21 chapters dealing with all phases of soldering. Combining the theoretical with the practical, the manual describes techniques in detail and provides instructions on how, when and what to solder. Topics covered include principles of soldering, joint design, equipment, processes and procedures, inspection and testing, and safety. In addition, a wide variety of metals used in soldering is discussed.

The list price of the SOLDERING MANUAL is \$6.00.* Send your orders for copies to the American Welding Society, 2501 N.W. 7th Street, Miami, Florida 33125.

*Discount 25% to A and B members; 20% to bookstores, public libraries, and schools; 15% to C and D members. Add 4% Sales Tax in Florida.

Appendix

The following tables present the range of properties studied for the various aluminum and titanium alloys indicated.

Table A1 — Characteristics of Aluminum Alloys Commercially Produced as 1 In. Thick Plate

Alloy	Temper	σ_{ys} , ksi	1 in. DT energy, ft-lb
2020	T651	76	90
2021	T8151	63.4	234
2024	T351	49	472
2024	T4	48	330
2024	T851	67.6	234
2219	T851	55	240
2219	T87	58	290
5083	O	19	1790
5086	H112	24	1480
5086	H116	27	1330
5086	H117	30	1832
5456	O	22.2	1454
5456	H116	31.2	714
5456	H117	32.5	1205
5456	H117	39.6	958
5456	H321	34	726
6061	T651	40	640
6061	T651	38	720
7005	T63	46	900
7075	T7351	66	210
7075	T6	78	120
7075	T6	75	71
7079	T6	75	93
7106	T63	53	490

Table A2 — Characteristics of Titanium Alloys Commercially Produced as 1 In. Thick Plate

Alloy	Nominal yield strength range, ksi	Nominal DT energy range, ft-lb
α Alloys		
Ti-5Al-2.5Sn	110-125	1500-1900
Ti-5Al-5Sn-5Zr	110-115	1000
Unalloyed	80	800
Near-α Alloys		
Ti-7Al-2Cb-1Ta	90-120	1600-3200
Ti-8Al-2Cb-1Ta	95-115	1500-3000
Ti-6Al-2Cb-1Ta-0.8Mo	95-120	1500-2500
Ti-6Al-2Cb-1Ta-1.2Mo	105-115	1200-1700
Ti-6.5Al-5Zr-1V	125	800
Ti-6Al-4Zr-2Sn-.5Mo-.5V	110-115	1500
Ti-6Al-4Sn-1V	130	1900
Ti-6Al-4Zr-1V	110	800
Ti-7Al-3Cb-2Sn	110	1500-1800
$\alpha + \beta$ Alloys		
Ti-6Al-4V	105-140	300-2990
Ti-6Al-2Mo	105-125	1200-2700
Ti-7Al-2.5Mo	100-120	1400-2600
Ti-7Al-1Mo-1V	105-115	800-1500
Ti-8Al-1Mo-1V	115-125	1000
Ti-6Al-4V-2Sn	120	1000
Ti-6Al-3V-1Mo	110-130	1000-2700
Ti-6Al-4V-2Mo	120-150	500-1100
Ti-6Al-2Sn-1Mo-1V	100	1900
Ti-6Al-4Zr-2Mo	120-135	700-1400
Ti-4Al-3Mo-1V	95-100	2000
Ti-6Al-6V-2Sn-1Cu-.5Fe	125-135	500-700
Ti-6Al-6V-2Sn-2Mo	125-175	300-600
Ti-5Al-2Sn-2Mo-2V	105-120	1100-2300
β Alloys		
Ti-11Mo-5Sn	90-100	3200-3600
Ti-11Mo-5.5Sn-5Zr	100-110	1800
Ti-10Mo-5.4Sn	115-135	1200-1600
Ti-2Al-4Mo-4Zr	90-100	2700-3100
Ti-3Al-3Mo-3Zr	90-100	1700
Ti-3Al-13V-11Cr	136	820

WRC Bulletin No. 190 December 1973

"Fluxes and Slags in Welding"

by C. E. Jackson

Prior to the publication of this interpretive report, users of covered electrodes, submerged-arc and other flux-controlled welding processes have had available little information or explanation of flux-slag technology. In spite of this lack of information for the user, application of welding processes utilizing fluxes has been extensive. The lack of available information has been due in part to the proprietary nature of flux formulations. Prof. Jackson, in his interpretive report, has unveiled the secrecy to provide the reader with a comprehensive review of the formulation and functions of welding fluxes and slags. It is hoped that a presentation of some of the principles of welding flux technology will provide an appreciation of improved quality of weld metal obtained through slag/metal reactions.

Publication of this paper was sponsored by the Interpretive Reports Committee of the Welding Research Council. The price of WRC Bulletin 190 is \$4.00 per copy. Orders should be sent to the Welding Research Council, 345 East 47th Street, New York, N.Y. 10017.

WRC
Bulletin
No. 107
Aug. 1965

(Reprinted April 1972)

Local Stresses in Spherical and Cylindrical Shells Due to External Loadings

by K. R. Wichman, A. G. Hopper and J. L. Mershon

Several years ago, the Pressure Vessel Research Committee sponsored an analytical and experimental research program aimed at providing methods of determining the stresses in pressure vessel nozzle connections subjected to various forms of external loading. The analytical portion of this work was accomplished by Prof. P. P. Bijlaard of Cornell University. Development of the theoretical solutions involved a number of simplifying assumptions, including the use of shallow shell theory for spherical vessels and flexible loading surfaces for cylindrical vessels. These circumstances limited the potential usefulness of the results to d_i/D_i ratios of perhaps 0.33 in the case of spherical shells and 0.25 in the case of cylindrical shells. Since no data were available for the larger diameter ratios, Prof. Bijlaard later supplied data, at the urging of the design engineers, for the values of $B = 0.375$ and 0.50 (d_i/D_i ratios approaching 0.60) for cylindrical shells. In so doing, Prof. Bijlaard included a specific warning concerning the possible limitations of these data.

Following completion of the theoretical work, experimental work was undertaken in an effort to verify the theory. Whereas this work seemingly provided reasonable verification of the theory, it was limited to relatively small d_i/D_i ratios—0.10 in the case of spherical shells and 0.126 in the case of cylindrical shells. Since virtually no data, either analytical or experimental, were available covering the larger diameter ratios, the Bureau of Ships sponsored a limited investigation of this problem in spheres, aimed at a particular design problem, and the Pressure Vessel Research Committee undertook a somewhat similar investigation in cylinders. Results of this work emphasized the limitations in Bijlaard's data on cylindrical shells, particularly as it applies to thin shells over the "extended range."

Incident to the use of Bijlaard's data for design purposes, it had become apparent that design engineers sometimes have difficulty in interpreting or properly applying this work. As a result of such experience, PVRC felt it desirable that all of Bijlaard's work be summarized in convenient, "cookbook" form to facilitate its use by design engineers. However, before this document could be issued, the above mentioned limitations became apparent presenting an unfortunate dilemma, viz., the data indicate that the data are partially inadequate, but the exact nature and magnitude of the error is not known, nor is any better analytical treatment of the problem available (for cylinders).

Under these circumstances, it was decided that the best course was to proceed with issuing the "cookbook," extending Bijlaard's curves as best as possible on the basis of available test data. This decision was based on the premise that all of the proposed changes would be toward the conservative (or "safe") side and that design engineers would continue to use Bijlaard's extended range data unless some alternative were offered. This paper was therefore presented in the hope that it would facilitate the use of Bijlaard's work by design engineers.

Since the paper was originally issued, a number of minor errors have been discovered and incorporated in revised printings as supplies were exhausted. The third revised printing was issued in April 1972.

The price of Bulletin No. 107 is \$3.00. Copies may be ordered from the Welding Research Council, 345 East 47th St., New York, N. Y. 10017.